The International Journal of Advanced Manufacturing Technology (2025) 141:6339–6346
https://doi.org/10.1007/s00170-025-17028-y

ORIGINAL ARTICLE

Inoculation process in gray cast iron and graphite expansion

Itamar Rodrigues de Lira[1,2,5] · Clécio Vicente da Silva[3] · João Antônio Lima Pacheco[1] · Edval Gonçalves de Araujo[1,2] · Moisés Euclides da Silva Junior[1,2] · Maurício David Martins das Neves[4] · Oscar Olimpio de Araujo Filho[1]

Received: 22 August 2025 / Accepted: 12 November 2025 / Published online: 28 November 2025

Abstract
The manufacturing of mill roller shells in gray cast iron demands rigorous control to ensure the integrity of the castings, wherein inoculation emerges as a critical metallurgical step. During solidification, inherent volumetric changes can lead to casting defects, most notably secondary shrinkage porosity. Before the experimental program, the rejection rate due to secondary shrinkage after riser cutting was 8% of the inspected castings; however, these parts were repurposed for other customers who specified a shorter length. This research analyzed the impact of inoculation process variables on graphite expansion during solidification, focusing on the reduction of shrinkage in mill roller shells. The experimental methodology evaluated the formation of primary and secondary shrinkage. After optimizing the conditions (experiment E), the occurrence of this defect was reduced to 0% in the validated mill roller shells (weighing between 3 and 30 tons), while maintaining the mechanical properties within the specification. This successful elimination of defects post-riser removal provides a robust methodology for predicting and controlling the process variables governing their formation.

Keywords Shrinkage · Gray cast iron · Inoculation · Graphitic expansion

1 Introduction

Gray cast iron is widely used in industry due to its remarkable properties, including high vibration damping capacity, good thermal conductivity, excellent machinability, ease of casting, and low production cost, making it a well-established choice for various applications. Its microstructural constituents, specifically morphology and the nature of metallic matrix, are the primary determinants of its mechanical properties. Among the variants of this material, the alloy with a fully pearlitic matrix and uniformly distributed type A graphite stands out for its superior properties and is the most produced globally [1–3].

The production flowchart for gray cast iron, illustrated in Fig. 1, begins with the melting of the metallic charge in a furnace to obtain the base molten metal. Subsequently, the liquid metal is poured into a first transfer ladle (kettle-type ladle) for the purpose of slag removal and temperature adjustment. Inoculation is performed during the transfer from the first to the second ladle (bottom-pour ladle). Following this, the post-inoculation step occurs during the pouring from the second ladle into the mold, where the metal solidifies and takes on the final shape of the desired part. As highlighted in Fig. 1, these last two steps are the most relevant stage for controlling graphite nucleation and, consequently, for managing the effects of contraction during the casting process.

In the sugar-alcohol industry, gray cast iron mill roller shells are vital components in juice extraction, but imperfections such as shrinkage cavities compromise their performance and durability [4]. These defects, typically revealed during final machining operations, are a direct consequence of inadequate liquid metal feeding to

✉ Itamar Rodrigues de Lira
itamar.lira@ufpe.br

1 Department of Mechanical Engineering, Universidade Federal de Pernambuco, Recife, Brazil

2 Brazilian Institute for Material Joining and Coating Tecnologies (INTM), Universidade Federal de Pernambuco, Recife, Brazil

3 Department of Mechanical Engineering, Estácio University Center, Recife, Brazil

4 Institute of Energy and Nuclear Research (IPEN), University of São Paulo, São Paulo, Brazil

5 Rua Manoel Soares de Souza, n° 19, Vitória de Santo Antão, São Vicente de Paulo, PE, Brazil

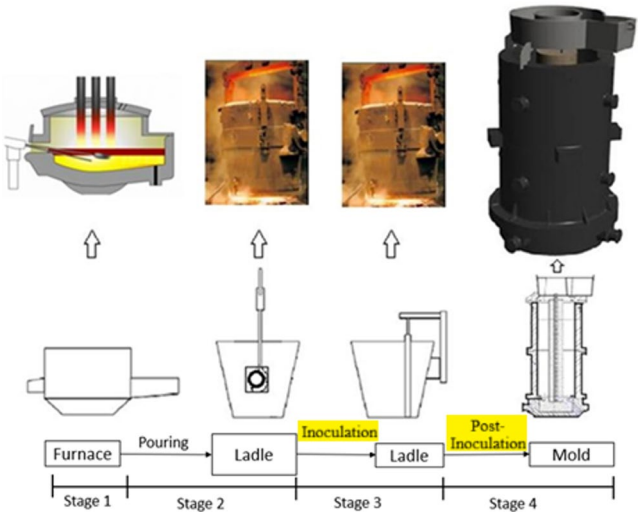

Fig. 1 Flow of the gray cast iron production process

compensate for solidification shrinkage. Process parameters such as inadequate riser dimensioning, inefficient feeding system design, excessive superheat, deficient inoculation, or a suboptimal carbon equivalent value are known contributing factors to this class of defect [4, 5, 7].

Despite extensive laboratory investigations on inoculation, graphite morphology, and contraction porosity, quantitative evidence at industrial scale for heavy-section gray cast iron remains scarce. In particular, documented elimination of secondary shrinkage after riser removal in 3–30 t castings via combined control of inoculation and riser solidification is seldom reported, leaving a practical gap between laboratory mechanisms and full-scale foundry practice [1–3, 8–13]. This study addresses this gap by adjusting the inoculation process parameters, in conjunction with riser solidification conditions, to eliminate secondary shrinkage in 3- to 30-ton gray cast iron mill roller shells. The primary objective is to reduce the defect rate after riser removal from a baseline of 8% to 0%, while ensuring the microstructure (predominantly Type A graphite) and mechanical properties (tensile strength and Brinell hardness) remain within specification.

2 Methodology

The experimental program was motivated by significant operational impacts, including rework, delivery delays, and capacity losses, stemming from a persistent issue with secondary shrinkage porosity. Before this investigation, the rejection rate for this defect, detected after riser removal, was 8% of inspected castings, which corresponded to the rejection of approximately 180 tons of mill roller shells over a two-month period. As these defects were not predicted by solidification simulations, their elimination became a priority. Consequently, efforts were focused on stabilizing the inoculation practice and optimizing the effects of graphitic expansion during solidification.

In this study, no direct measurement of the resulting volumetric expansion was performed. Instead, its effects were identified and inferred indirectly based on a combination of factors: the elimination of shrinkage defects after riser removal; the microstructural correlation, evidenced by an increase in eutectic cells and a predominance of Type A graphite over undercooled Type D; and the implementation of process conditions that favor the thermal closure of the riser and the action of expansion pressure on the casting body, such as the removal of exothermic powder, adjustment of the riser-to-part mass ratio, and manual control of the pouring process.

2.1 Alloy composition and mechanical properties specification

Table 1 presents the specification of the chemical composition and mechanical properties, such as tensile strength (TS) and Brinell hardness (HB), for gray cast iron, including the minimum and maximum allowable values for each element and property.

2.2 Description of defects

In gray cast iron mill roller shells, compared to a riser without irregularities (Fig. 2A), anomalies characterized by metal expansion or reaction in the riser were observed (Fig. 2B and C), resulting in secondary shrinkage cavities visible after riser cutting (Fig. 2D). These imperfections lead to part rejection, increasing production costs and impacting delivery deadlines.

Table 1 Specification of the chemical composition and mechanical properties of Gray cast iron

	%C	%Si	%Mn	%*P*	%S	%Cr	%S	Ceq	RT	Hardness
									kgf/mm^2	HB
Minimum	2,80	1,60	0,50	-	0,06	0,12	0,12	3,34	22	180
Maximum	3,10	1,80	0,70	0,15	0,12	0,30	0,30	3,78	-	230

Fig. 2 Mill roller shells showing a riser without defect (**A**) and expanded riser (**B** and **C**). Mill sleeve with the riser removed, displaying a secondary shrinkage defect (**D**)

Two samples, referred to as sleeves No. 01 and No. 02, were obtained from the upper region of two mill roller shells cast using the standard process (Table 2), which exhibited secondary shrinkage cavities after riser removal. Sampling was conducted following the conventional protocol, with no modifications to the molten metal preparation process.

2.3 Thermal monitoring

In the studied industrial process, all runs underwent standardized thermal monitoring. Temperature measurements (pouring, inoculation, post-inoculation, and final) were taken with an immersion thermocouple before casting and recorded on a process sheet. This sequential data allowed for the tracking of superheat and temperature variations resulting from transfers and holding times, minimizing thermal fluctuations that could mask the effects of the inoculation and post-inoculation variables.

2.4 Experimental design and evaluation criteria

This study was structured as an empirical industrial trial, comprising five process experiments (A–E), with each experiment applied to 10 castings of the same component. The primary response was binary, defined by the presence or absence of secondary shrinkage after riser removal. This primary evaluation criterion was operational (accept/reject), consistent with the industrial decision-making process for part rejection and directly addressing the research question of whether secondary shrinkage could be eliminated.

For consistency, a standardized visual inspection protocol was employed, utilizing uniform lighting, distance, and angle, with photographic records maintained for each part. When a defect was identified, a secondary analysis was performed: its largest projected dimension (in mm) and projected area were measured using ImageJ software. This measured area was then expressed as a fraction of the inspected surface zone to standardize the defect's severity for comparative purposes.

2.5 Microstructural characterization

Samples for microstructural analysis were taken from the upper region of the mill roller shells, after riser removal, and prepared according to ASTM E3. The preparation sequence involved grinding with SiC papers (#220, #320, #600, #1200) followed by polishing with diamond suspensions (6 µm, 3 µm, and 1 µm). Observations of graphite morphology and size were conducted on unetched samples, following the ASTM A247-10 standard. To reveal the metallic matrix (pearlite/ferrite), the samples were etched

Table 2 Conducted experiments

Experiments	Inoculant	Post-inoculant	Exothermic powder/Rice husk	Riser/Part (%)	Ladle type	Objective
Standard	0.6% IMB75%	Yes	Exothermic Powder	9	Mechanical (overhead crane)	Reference
A	0.6% FeSi75%	Yes	Exothermic Powder	9	Mechanical (overhead crane)	Evaluate the influence of inoculant type
B	0.5% IMB75%	No	Exothermic Powder	9	Mechanical (overhead crane)	Reduce the effect of excessive graphitization
C	0.6% IMB75%	No	Rice Husk	11	Mechanical (overhead crane)	Decrease exothermic effect in the riser, prevent secondary shrinkage from reaching the part
D	0.6% IMB75%	Yes	No	11	Mechanical (overhead crane)	Contain expansion in risers of sleeves > 22 tons
E	0.6% IMB75%	Yes	No	11	Manual (kettle type)	Contain expansion in risers of sleeves > 22 tons, with manual pouring control and inoculant addition

with 2% Nital for 5–10 s, followed by immediate rinsing and drying. The matrix fraction was estimated using image analysis (LECO) and verified by visual field assessment. Optical microscopy was performed using a Zeiss Neophot 32 microscope at typical magnifications of 25X and 100X; where necessary, multi-field phase analysis was conducted. All measurements were repeated by two evaluators to ensure consistency.

2.6 Experimental plan

The standard production process for mill roller shells employed 0.6% IMB75% inoculant (chemical composition: 74–79% Si; 0.8–1.2% Ca; 0.8–1.2% Ba; <1.2% Al; particle size: 2.38 × 6.35 mm), supplemented by 0.06% post-inoculant (FeSi75% powder) during pouring. Additionally, FERRUX 707E FOSECO-VESUVIUS exothermic powder was used, and the mass ratio riser/part was 9%. Pouring was performed using a ladle operated by an overhead crane.

Five experiments were conducted (Table 2 – tests A to E), in which variables related to the standard process (Table 2 – Standard) were modified. The modifications included the quantity and type of inoculant, the presence or absence of post-inoculant, the use or non-use of "exothermic powder" or "rice husk" (as thermal insulator) applied after pouring, the mass ratio riser/part, and the type of pouring ladle. Each variation was implemented starting from the standard process and applied to ten castings of the same component, aiming to observe defect occurrence. Mill roller shells were carefully selected so that, if shrinkage cavities appeared after riser removal, the part could be repurposed for other dimensional specifications, considering the defect is located in the upper region of the casting.

3 Results and discussion

The structure, quality, and mechanical properties of gray cast iron are intrinsically determined by chemical composition, cooling rate, and, decisively, by the inoculation treatment [14–16]. In the manufacturing of this material, primary shrinkage is conventionally controlled by properly sized risers and feeding channels. Conversely, secondary shrinkage originates in thermally isolated interdendritic liquid pools within the casting's thermal center (hot spot), resulting from solidification under a negative pressure gradient due to insufficient feeding [17, 18]. Therefore, top risers are required to compensate for the initial contraction of the liquid metal, while residual solidification contractions are mitigated by graphite expansion itself.

Inoculation is an essential treatment performed immediately before pouring that optimizes graphite formation during solidification. This process refines the microstructure by increasing nucleation sites, reducing carbide formation, and improving graphite distribution and type, resulting in higher density and superior mechanical properties such as tensile strength and wear resistance. However, inoculation directly influences the formation of secondary shrinkage cavities. By increasing the number of nucleation sites, it reduces undercooling and alters phase growth kinetics, promoting a more pasty solidification with a higher number of eutectic cells [2, 11]. This promotes the formation of a finer, more complex network of interdendritic channels, which increases the resistance to interdendritic feeding, thereby impeding the flow of residual liquid from the riser. It is important to note that both insufficient inoculation which promotes cementite formation and intensifies secondary contraction and excessive inoculation which results in overly pasty solidification increase the tendency to secondary shrinkage defects [5, 12].

Cast irons with an equivalent carbon content (Ceq) above 3.7% exhibit self-feeding capacity, as graphite expansion during solidification compensates for liquid metal contraction, minimizing porosity and shrinkage [13]. However, the Ceq of the mill roller shells in question is significantly below the recommended level and, in some operational runs, falls below the 3.7% threshold. This reduced Ceq compromises the self-feeding capacity and the contribution of graphitic expansion, making the observed effects particularly sensitive to the inoculation practice and the solidification state of the riser.

The effectiveness of this process depends directly on the quality of inoculation, which controls the formation and development of graphite flakes, refining the microstructure and improving the structural integrity of cast parts. Additionally, variations in graphite morphology can contribute to the formation of shrinkage porosity; cast irons with Type D graphite, formed under high undercooling conditions, exhibit lower self-feeding capacity compared to Type A graphite, impacting contraction compensation and potentially leading to defects in components such as mill roller shells [6, 17].

Morphological analysis of porosity in gray cast iron mill roller shells is essential to understand cavity formation. In samples produced using the standard procedure (Table 2), the main defect identified was secondary shrinkage cavities, evidenced in Figs. 3A and 4A. The predominant microstructure in these castings was characterized by the presence of undercooled (Type D) graphite morphology. These cavities form during secondary contraction, a process regulated by solidification of the remaining liquid between dendrites [6, 17].

The micrograph of mill sleeve No. 01 (Fig. 3) revealed a matrix of 97% pearlite and 3% ferrite (Class VII, Types

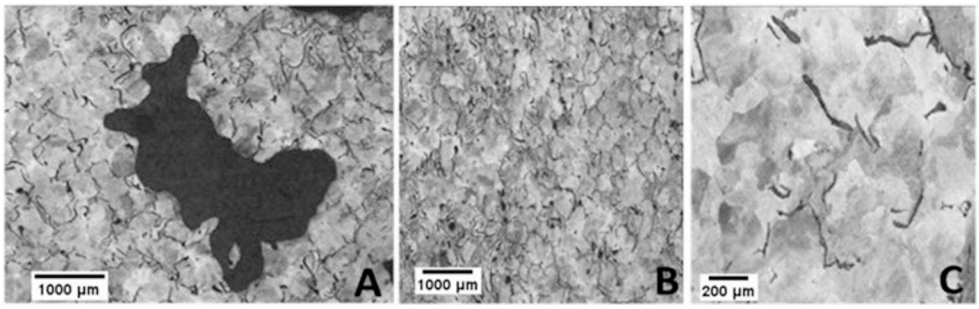

Fig. 3 Micrography of mill sleeve No. 01 showing shrinkage with irregular morphology (**A**), Type A and D graphite, magnifications of 25x (**A** and **B**) and 100x (**C**), optical microscopy. Nital 2%

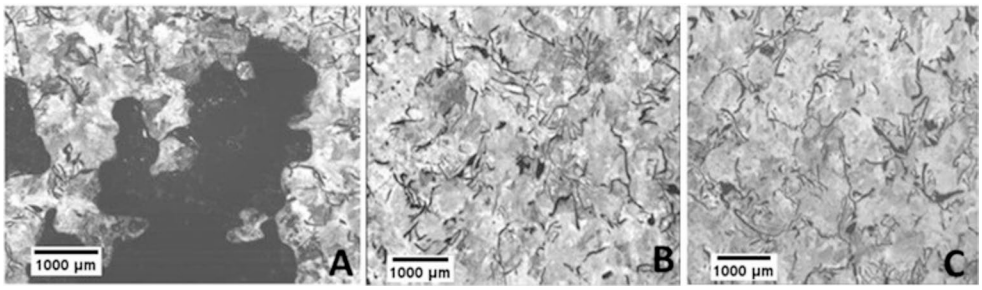

Fig. 4 Micrography of mill sleeve No. 02 showing shrinkage with irregular morphology (**A**), predominantly Type D graphite (**B** and **C**), magnification 25x. Nital 2%

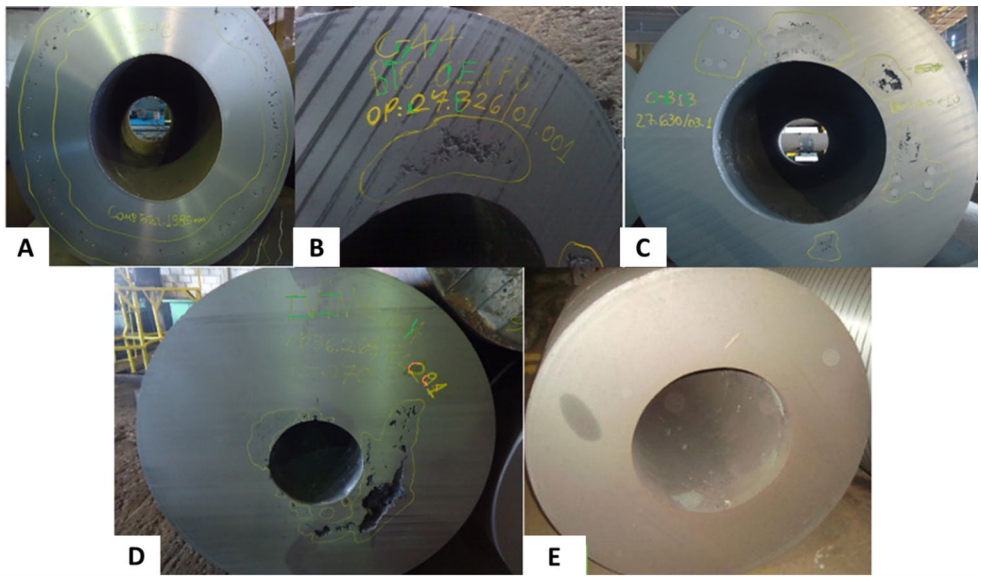

Fig. 5 Surface images of mill roller shells from experiments **A**, **B**, **C**, **D**, and **E** after riser removal

Table 3 Tensile strength and hardness results for experiments A, B, C, D, and E

Experiment	Tensile strength (kgf/mm²)	Hardness (HBN)
A	29,0±3	210±8
B	27,2±2	206±7
C	30,6±3	205±10
D	30,3±2	203±7
E	31,2±3	205±8

A and D graphite, Size 4, ASTM A247-10), with irregular porosity. Sleeve No. 02 (Fig. 4) showed microstructures with variable matrix compositions (73% pearlite/27% ferrite or 97% pearlite/3% ferrite), predominantly Type D graphite (Size 4–5), and small distributed porosities.

With the objective of optimizing the production process and manufacturing gray cast iron mill roller shells free of shrinkage defects, modifications were implemented focusing on effective control of expansion and solidification in the riser region. The sleeves were inspected after riser removal, and one piece per experiment was documented photographically (Fig. 5), with the resulting mechanical properties detailed in Table 3.

In Experiments A and B, changes in the inoculation procedure (type or amount of inoculant) were tested, maintaining the addition of exothermic powder and a riser/part ratio of 9%. However, all castings in these trials showed shrinkage defects after riser removal (Fig. 5A and B).

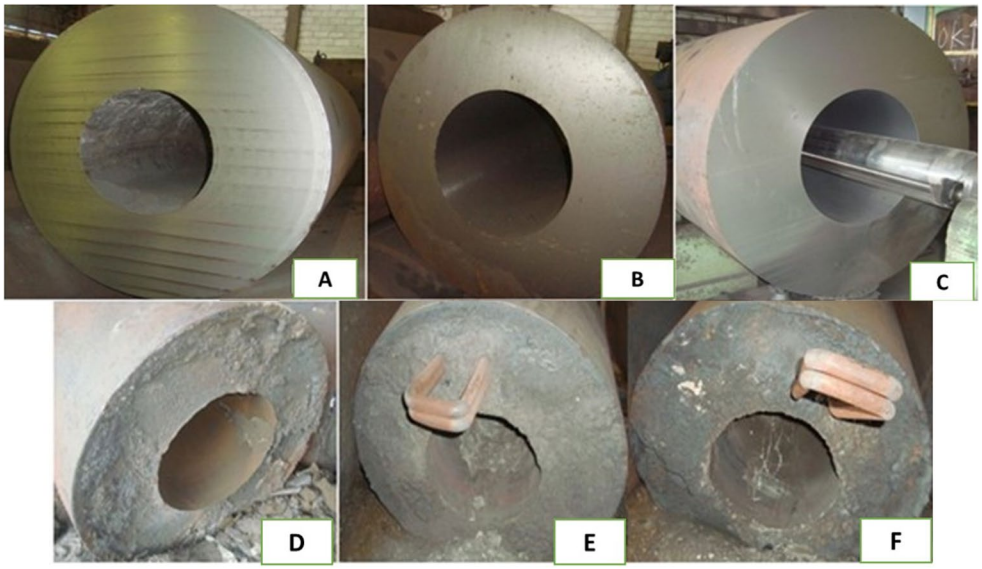

Fig. 6 Mill roller shells (**A**, **B**, and **C**) with risers removed, showing absence of secondary shrinkage. Mill roller shells (**D**, **E**, and **F**) without defects in the riser region

In Experiment C, the absence of post-inoculant and the use of rice husk as insulating material, along with an increased riser/part ratio to 11%, resulted in the elimination of defects in sleeves weighing less than 22 tons. However, the problem persisted in heavier parts (Fig. 5C).

In Experiment D, with standard inoculation and post-inoculation, no use of exothermic powder or rice husk, and a riser/part ratio of 11% without exothermic powder, secondary shrinkage was reduced in sleeves below 22 tons. However, pronounced primary shrinkage was present in sleeves over 22 tons, extending into the casting itself (Fig. 5D), in addition to secondary shrinkage.

In Experiment E, the elimination of secondary shrinkage defects (Fig. 5E) was achieved by combining standard inoculation and post-inoculation, without the use of exothermic powder or insulation, increasing the riser/part ratio to 11%, and using a kettle-type ladle operated manually. Figure 6 illustrates examples of mill roller shells without secondary shrinkage after riser removal (6 A, 6B, 6 C) and the integrity of the riser region before removal (6D, 6E, 6 F).

The modification in ladle type, which provided greater control over metal flow and inoculant addition, was key to the success of Experiment E. In casting processes, early solidification of the "neck" section in the riser system is crucial to facilitate graphite expansion and ensure effective feeding of the casting. However, the riser design in the mill roller shells used lacks a neck, making this configuration critical.

The solidification behavior of the riser region is influenced by the alloy's nucleation level, with higher nucleation rates promoting earlier graphite expansion. Previously, the use of exothermic powder kept the riser liquid, allowing metal flow driven by graphite expansion to escape through the riser due to the absence of a neck. The discontinuation of exothermic powder was therefore a strategic measure to accelerate riser solidification, ensuring graphite expansion effectively acts on the casting and contributing to the elimination of secondary shrinkage defects.

Despite the occurrence of shrinkage defects in some experimental conditions (A, B, C, and D), the tensile strength and hardness properties of all tested parts, including the intact part from Experiment E, remained within the limits specified in Table 1, as shown in Table 3.

4 Discussion of the mechanism

The successful elimination of secondary shrinkage in Experiment E can be explained by the interplay between graphite expansion and riser solidification dynamics. In gray cast iron, the eutectic expansion of graphite generates a positive pressure that compensates for liquid contraction. For this pressure to act effectively within the casting body, the feeding zone (riser) must not remain liquid for too long; otherwise, the liquid metal is expelled back through the riser, a phenomenon exacerbated by the absence of a neck in the riser design.

The use of exothermic powder keeps the riser liquid for an extended period, delaying the formation of a solid "cap" on its surface. By removing the exothermic powder and marginally increasing the riser-to-part mass ratio, we promoted a faster solidification of the upper riser region. This created a rigid barrier that redirected the expansion pressure inward, into the casting, effectively closing interdendritic voids.

Furthermore, manual pouring control with a kettle-type ladle allowed for better regulation of the metal stream and the addition of the inoculant. This fine-tuned the nucleation level, promoting a higher eutectic cell count and reducing

undercooling, which maintained sufficient permeability for local feeding until the expansion pressure could act effectively. The delicate balance between sufficient nucleation (to avoid cementite and Type D graphite) and the thermal condition of the riser (without exothermic powder) explains why only the specific combination of factors in Experiment E led to the complete elimination of secondary shrinkage after riser removal.

5 Conclusions

Based on the results of this industrial trial, the following conclusions can be drawn:

1. Under full-scale foundry conditions, the occurrence of secondary shrinkage after riser removal was reduced from a historical 8% rejection rate to 0% in the validated process experiment (Experiment E; $n = 10$), while tensile strength and Brinell hardness remained within specification. This directly links the presence or absence of the defect to the specific inoculation and feeding conditions tested.
2. Across the different experiments, the elimination of secondary shrinkage coincided with a predominantly Type-A graphite morphology (ASTM A247), in contrast to the undercooled Type-D graphite observed in defective castings. This microstructural shift is consistent with improved feeding during eutectic solidification. As in-situ dilatometry was not performed, graphite expansion was inferred operationally from: (i) the elimination of defects after riser removal, (ii) the resulting graphite morphology, and (iii) the implementation of process conditions that promoted accelerated riser solidification.
3. Variations in inoculant type or dosage alone did not directly correlate with the defect rate. The beneficial effect of inoculation was conditional on the riser solidification state and pouring control, a conclusion supported by the comparison across experiments (A–E). This highlights that the solution is not universal but depends on a validated combination of parameters.
4. The validated process for heavy-Sects. (3–30 t) gray cast-iron roller shells combined: standard inoculation plus post-inoculation, removal of exothermic powder from the riser, an increase of the riser-to-part mass ratio to ~11%, and manual kettle pouring. In this configuration (Experiment E), secondary shrinkage was not observed in any of the inspected castings ($n = 10$), and all mechanical properties met the required specifications.
5. The suppression of exothermic powder likely accelerated the riser's solidification, creating an earlier solid "cap" and promoting the transfer of graphite expansion pressure into the casting rather than allowing it to vent through the riser. This interpretation is consistent with the observed defect elimination and microstructural evidence but should be viewed as plant-validated operational guidance, not as a universal prescription for all casting geometries and alloys.
6. The validated parameters from this study provide a transferable, shop-floor-oriented methodology for similar heavy-section castings. Further academic work, such as in-situ dilatometry and EDS/micro-segregation mapping, could deepen the understanding of microchemical causality without altering the practical industrial outcome achieved, which successfully reduced the defect rate from 8% to 0%.

Declarations

Competing interest The authors declare that they have no known competing financial interests or personal relationships that could have appeared to influence the work reported in this paper.

References

1. Riposan I, Chisamera M, Stan S (2014) New developments in high quality grey cast irons. China Foundry 11:351–364
2. Stefanescu DM (2017) Cast Iron Science and Technology. ASM International
3. Wang G, Chen X, Li Y, Liu Z (2018) Effects of inoculation on the pearlitic gray cast iron with high thermal conductivity and tensile strength. Materials 11(10):1876. https://doi.org/10.3390/ma11101876
4. Fuoco R (1990) Princípios de alimentação de ferros Fundidos cinzentos e nodulares. In: Curso Alimentação e Enchimento de Moldes. São Paulo
5. Ecob CM (2005) A review of common metallurgical defects in ductile cast iron. Elkem AS, Foundry Products Division
6. Guesser WL (2009) Propriedades mecânicas dos ferros fundidos (1ª ed.). Blucher
7. Tadesse A, Fredriksson H (2017) Volume change during the solidification of grey cast iron: its relation with the microstructural variation, comparison between experimental and theoretical analysis. Int J Cast Met Res 30(3):159–170. https://doi.org/10.1080/13640461.2016.1277851
8. Tadesse A, Fredriksson H (2014) The effect of inoculation on the thermal expansion/contraction during solidification of Gray cast iron. Mater Sci Forum 790–791, 447–451
9. Tadesse A, Fredriksson H (2015) Experimental studies of gray cast iron solidification with Linear Variable Differential Transformer. In Nastac L, Baicheng L, Hasse F (eds) Advances in the science and engineering of casting solidification: an MPMD symposium honoring Doru Michael Stefanescu. Wiley, pp 305–312
10. Szczęsny A, Kopyciński D, Guzik E (2022) Inoculation of gray cast iron intended for large scale and heavy weight castings of bottom plates and counterweights manufactured in the Krakodlew S.A. Arch Foundry Eng 22(3):19–24
11. Merchant HD, Wallance JF (1960) Inoculation effect on risering of gray iron. AFS Trans 68:429–439
12. Alonso G, Stefanescu DM, Suarez R, Loizaga A, Zarrabeitia G (2014) Kinetics of graphite expansion during eutectic

solidification of cast iron. Int J Cast Met Res. https://doi.org/10.1179/1743133613Y.0000000085
13. Bartocha D, Janerka K, Suchon J (2005) J Mater Process Technol 162–163:465–470
14. Hermanth J, Rao KVS (1999) J Mater Eng Perform 8(4):417–423
15. Xu W, Ferry M, Wang Y (2005) <article-title update="“added”>Influence of alloying elements on as-cast microstructure and strength of gray iron. Mater Sci Eng A 390(1–2):326–333
16. Fuoco R et al (1995) Rechupes Devido à contração Em ferros Fundidos cinzentos. CONAF 1995 – Congresso de Fundição. São Paulo, pp 441–454
17. Fuoco R, Corrêa ER, Cavalcanti AH (2007) Caracterização de Porosidades Em ferros Fundidos cinzentos e nodulares. CONAF 2007 – Congresso de Fundição. São Paulo, pp 1–23
18. Fuoco R (2002) Modo de solidificação e técnicas de alimentação de ferros Fundidos cinzentos e nodulares. Pós-graduação em Engenharia de Fundição – Instituto de Pesquisas Tecnológicas